32nd Electric Vehicle Symposium (EVS32)
Lyon, France, May 19 - 22, 2019

Innovative and Highly Integrated Modular Electric Drivetrain

Jonas Hemsen[1], Daniel Kieninger[1], Univ.-Prof. Dr.-Ing. L. Eckstein[1], Mathias R. Lidberg[2], Dr. ir. H. Huisman[3], Prof. Dr. E.A. Lomonova[3], Daniel Oeschger[4], Charley Lanneluc[5], Olivier Tosoni[5], Patrick Debal[6], Michael Ernstorfer[7], Rémi Mongellaz[8]

[1]*Institute for automotive engineering – RWTH Aachen University, jonas.hemsen@ika.rwth-aachen.de*

[2]*Mechanics and Maritime Sciences - Chalmers University of Technology, mathias.lidberg@chalmers.se*

[3]*Electromechanics and Power Electronics Group - Eindhoven University of Technology, h.huisman@tue.nl*

[4]*BRUSA Elektronik AG, daniel.oeschger@brusa.biz*

[5]*Commissariat à l'énergie atomique et aux énergies alternatives – CEA, charley.lanneluc@cea.fr*

[6]*Punch Powertrain, patrick.debal@punchpowertrain.com*

[7] *MAHLE ZG Transmissions GmbH, ernstorfer@zg-gmbh.de*

[8]*Simulations and Test Solutions – Siemens Industry Software, S.A.S., Lyon, remi.mongellaz@siemens.com*

Summary

A highly integrated electric drivetrain module is presented. The drivetrain is modular and incorporates novel technologies for the driveline components: high ratio, dual speed transmission, high speed electric machine and gallium nitride power electronics. The integration of these components into one single housing makes the drive module flexible to use with both conventional and alternative propulsion technologies. Several hybrid- and electric drivetrain topologies can be realized. The holistic approach of the engineering process of these components yields benefits in terms of sizing, costs and losses, leading to a compact, efficient and easy to integrate drivetrain module.

Keywords: Electric drive, optimization, permanent magnet motor, inverter, transmission

1 Introduction

Electrification of passenger cars and light-duty vehicles – which are still responsible for around 20% of Europe's greenhouse gas emissions [1] - will have an enormous effect on the reduction of greenhouse gas emissions. Additionally, pollutant-free air in dense urban areas is possible with electrified propulsion. However, the maturity of electric drives needs a final push for better performance and efficiency so that battery capacity can be saved and driving range can be increased. Combined with a cost reduction, a massive adoption of such transport in Europe and worldwide can be generated. This paper presents a new generation of a modular electric drive module, which can be used for various configurations of Full- and Hybrid Electric Vehicles. Focus is on cost reduction, low environmental impact, efficiency, and mass manufacturing readiness. The multiphase electric machine based on permanent magnets will be combined with the latest Gallium Nitride (GaN) power switches, advanced control with higher fault tolerance, and cooling features

with reduced dimensions and higher efficiency. It will be linked with a performant two-speed transmission, adapting also new regenerative braking strategies. The development takes industrial- and user requirements into account as well as environmental impacts through life cycle analysis, to gear the activities towards a full vehicle design approach and the realization of each component and the complete powertrain. The project gathers nine cutting-edge partners from the fields of automotive, power electronics, transmissions and electric motors including three research centres, three Tier-1 suppliers and “Small and Medium Entrepreneurs”.

2 Permanent Magnet Hybrid Synchronous Machine

2.1 Machine Design

In order to achieve very high power densities even with low available current and voltage, sophisticated electromagnetic designs are required. Additionally, the automotive market has special requirements which adds additional effort to the design of a motor which is safe and strong at the same time. To meet these challenges, the Hybrid Synchronous Motor (HSM) was invented a few years ago which is an evolution of the internal permanent magnet motor (IPM). It is called Hybrid, because it utilizes the combination of reluctance- and electromagnetic torque. The torque production by these two effects is the reason, why it is difficult to design such machine type. Small changes in the geometry or materials have influence on both effects and therefore can have significant impact on performance, torque ripple, efficiency, power factor, controllability, demagnetisation and more.

The main goal for the EM development was to save more than 50 % magnet mass compared to existing PMSM with similar power, to reduce the active weight and to improve the efficiency. Many iterations were needed to satisfy all of the previously defined drive requirements.

The resulting electric machine is a 6 pole, 6 phase HSM for high speeds up to 22500 rpm. Since power is proportional to both speed and torque, the torque demand for the peak power of 101 kW @ 6600 rpm is as low as 145 Nm. For decent accelerations from 0 to 50 km/h of a C-class vehicle with the given gear ratio of 21.65, a max. torque of 150 Nm is required. With this gear ratio and motor torque the vehicle can accelerate from 0 to 50 km/h in around 3 seconds.

As the required motor torque is fairly low, the required phase current is also low, in this case only 225 A (rms) per phase. A challenge for high speed motors are the centrifugal forces at the rotor which require mechanical stabilization and special rotor geometries to hold the permanent magnets in place.

The stator windings are made from a special wire type called “Formed Litz Wire” (FLW, fig. 1). This wire type provides low DC resistance (similar to massive copper bars) and low AC resistance (similar to conventional Litz wires) at the same time [2]. FLW technology combined with the high speed motor concept leads to a very low phase resistance and high continuous power, because a small motor has also short wires. Additionally, iron losses are reduced because of the low flux harmonic content, even if the motor speed is very high.

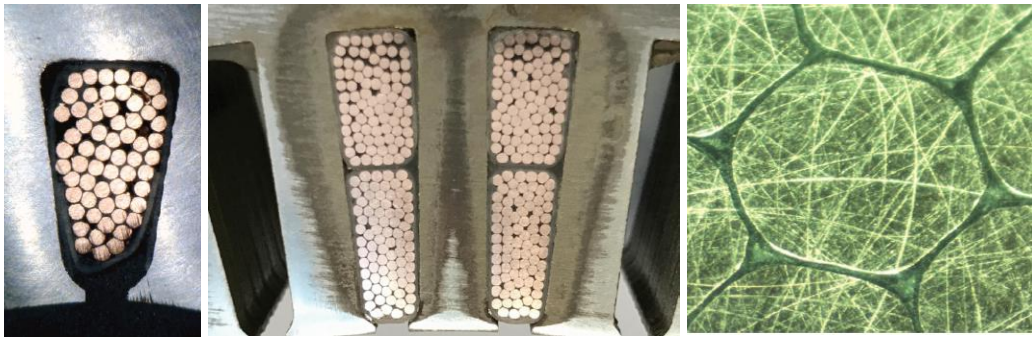

Figure 1: Classical Litz wire (left) and FLW (center) in stator slot and microscopic view of FLW (right) [2]

The project target torque of 150 Nm is surpassed from the simulations by 156 Nm at a current of 225 A (rms) and 320 VDC. Since the nominal speed will also be higher than expected (8650 rpm instead of 6600 rpm) the power at the new nominal speed rises to 141 kW. Above the nominal speed the power does not drop, it

rises again to more than 157 kW (213 hp) between 12000 and 16000 rpm. This is very impressive if we consider the low remanence flux density (B_r) of only 0.75 T @ 25°C, compared to sintered magnets which are available with more than 1.4 T @ 25°C.
To achieve these high levels of power with only 320 VDC and 225 A (rms), perfect magnetisation, optimal motor control and also very good mechanical design such as low friction bearings, a stiff shaft and many other intelligent features are needed.

At the end of the day not only a strong and light motor is strived for, it is no less important to have a good efficiency. Simulations showed that also with this high-speed drive, peak efficiency of more than 97 % can be realized (fig. 2). However, the key to save energy and battery size is mainly not peak efficiency, but a high drive cycle efficiency. Since the majority of drive cycles demand only low power, the good efficiency of this HSM design in the low-load areas helps to improve the overall energy consumption and to save battery capacity.

Efficiency [%] including winding, iron and bearing losses

Torque [Nm] \ Speed [rpm]	250	500	1000	2000	3000	4000	5000	6000	7000	8000	9000	10000	12500	15000	17500	20000	22500
160	54,82	70,73	82,66	90,16	92,88	94,25	95,04	95,55	95,89	96,12							
140	57,75	73,11	84,26	91,08	93,52	94,72	95,41	95,85	96,13	96,32	96,41	96,10					
120	60,86	75,55	85,85	91,98	94,13	95,17	95,76	96,12	96,35	96,50	96,60	96,42					
100	64,21	78,07	87,43	92,86	94,71	95,60	96,08	96,37	96,55	96,66	96,72	96,68	95,81				
80	67,79	80,65	89,01	93,71	95,27	96,00	96,38	96,60	96,72	96,78	96,81	96,83	96,35	95,30	93,77		
60	71,74	83,37	90,61	94,55	95,80	96,36	96,64	96,78	96,84	96,86	96,84	96,81	96,73	96,13	95,18	93,89	92,10
40	76,09	86,22	92,25	95,39	96,35	96,74	96,91	96,98	96,99	96,96	96,91	96,85	96,90	96,69	96,21	95,47	94,58
20	81,55	89,61	94,13	96,35	96,96	97,17	97,22	97,20	97,14	97,06	96,97	96,87	96,61	96,55	96,70	96,40	95,84
15	83,51	90,75	94,71	96,59	97,05	97,18	97,17	97,11	97,01	96,90	96,78	96,65	96,33	96,01	96,23	96,44	96,08
10	86,32	92,35	95,51	96,89	97,16	97,17	97,08	96,94	96,79	96,63	96,47	96,30	95,89	95,49	95,11	95,70	95,65
5	90,88	94,73	96,50	96,99	96,85	96,58	96,27	95,96	95,66	95,36	95,06	94,78	94,10	93,46	92,86	92,28	92,55

Figure 2: Simulated efficiency map of HSM

With an active weight of less than 30 kg the developed motor leads to a powertrain with a high power density and very low amount of rare earths.

2.2 Magnet Injection Moulding

Injection moulding of polymer-bonded magnets in the rotor cavities instead of insertion of sintered magnets was identified as one of the possible ways to further reduce the content of critical raw materials in the motor. Unfortunately, bonded magnets have less remanence flux density (B_r) than sintered magnets but they contain no heavy rare-earth (which is more critical than Nd and whose price might raise more severely if a supply crisis were to occur). They also allow complete freedom in the shape of the magnets, yielding some magnetic optimization potential of the rotor. Furthermore, all of the 66 magnets of a rotor slice can be injected in one single step which lowers production effort.

As the mechanical strength of bonded magnets is lower than of sintered magnets, centrifugal forces can be an issue. Hence, a mechanically stable rotor geometry has been developed for which the calculated power and efficiency of this injected magnet rotor is comparable to the sintered magnet one. Magnetostatic finite-elements calculations are now being performed in order to design a magnetizer tool to produce the proper magnetic field in the rotor cavities during the injection process (fig.3, left). With regards to materials, several grades of composites are available; the most suited one has been identified and injected to parallelepipedic samples (fig.3, right). The mould allows a magnetic field tuning in order to precisely reveal the field-dependence of magnetic properties and to allow further optimization of the injection mould.

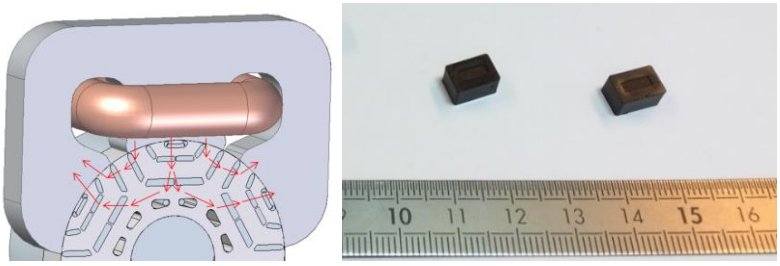

Figure 3: Principle of rotor magnetization (left) and injected magnet samples (right)

3 GaN Inverter

3.1 Advantages of Gallium Nitride Devices

The low voltage Gallium Nitride (GaN) power device technology (650 V) provides a lot of advantages compared to its Silicon (Si) and Silicon Carbide (SiC) competitors [3, 4]. In terms of performance, the Gallium Nitride devices have:

- an unrivalled switching performance with switching on/off in less than 10 ns,
- a low package inductance,
- a low on-resistance
- and reduced switching losses: 5 times better than Si devices and 2 times better than SiC devices.

With these advantages, the switching frequency can be raised and hence the size of passive components can be reduced: the inverter becomes smaller and more efficient at the same time. In terms of costs, fig. 4 shows that a Gallium(III) trioxide (Ga_2O_3) wafer is 3 times less expensive than a SiC one and it can be further reduced [5].

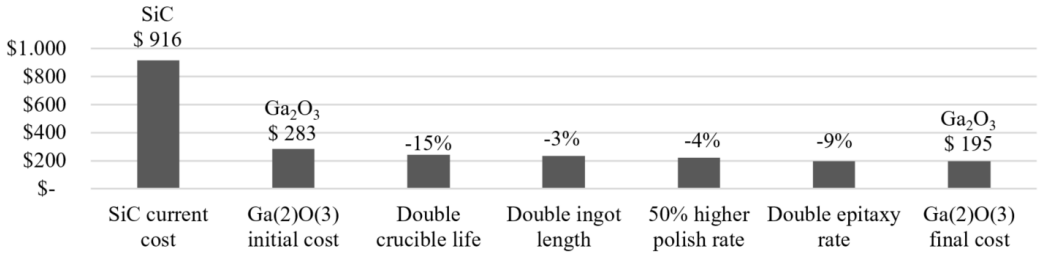

Figure 4: Costs comparison for Ga_2O_3 and SiC wafers [5]

The GaN technology is young and under ongoing development. As an example, the current capacity per die is still low: 60 A in 2017 and 120 A in 2019. In the framework of this research project, in order to fulfil power requirements, extensive work has been put in developing a reliable parallelization of dies.

3.2 GaN Power Board Conception

To obtain the required torque of 150 Nm in the 6-phase high speed motor, a current of 225 A (rms) per phase is requested. Each phase is independently connected to a full bridge in which each of two switches is realized with four parallelized GaN devices as specified in [6]. The topology of the full bridge is depicted in fig. 5 (left) with each switch ($K_{1,2,3,4}$) realized by four GaN devices in parallel. A first power board prototype of one leg of the bridge is shown in fig. 5 (right).

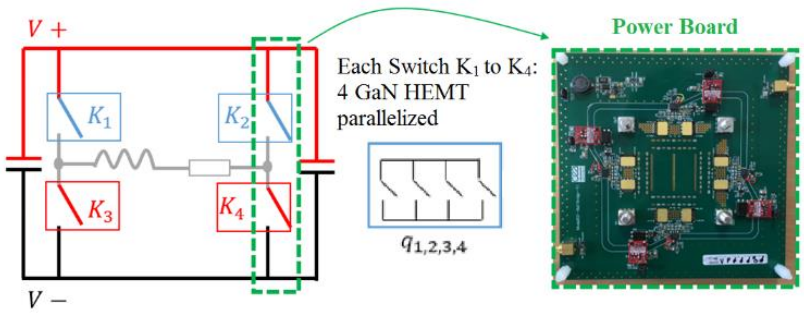

Figure 5: Topology of the power board (left) and first prototype (right)

Hardware development started with the parallelization of two devices. The experimental waveforms in fig. 6 show the results for two parallelized GaN devices with $V_{DC} = 300\,V$ at double pulse test with an inductive load ($L = 330\,uH,\ i_{sat} = 200A$). As can be shown, the switching of the two devices is synchronous which is essential to maintain an equal current in the two of them. Also, oscillations on the DC bus at a frequency of

approximately 1.2 MHz could be observed, which are induced by an exchange of reactive energy between the required decoupling capacitors.

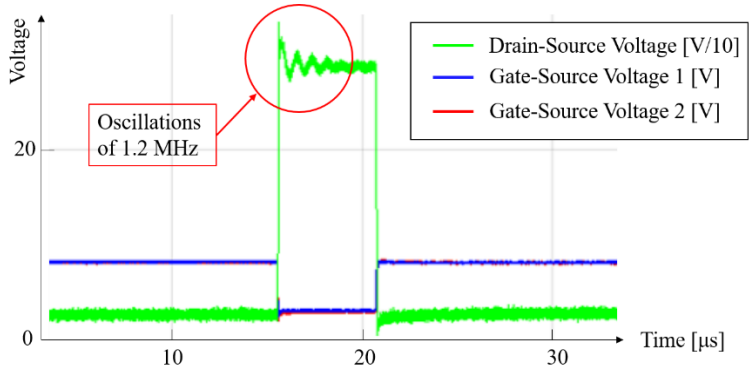

Figure 6: Experimental waveforms for 2 parallelized GaN devices

The oscillations can be explained by the characterization of the circuit using a Bode plot shown in fig. 7. A resonance can be observed at 1.2 MHz, matching exactly the frequency of the oscillations. These oscillations have been subsequently reduced by a better dimensioning of the decoupling and DC bus capacitors.

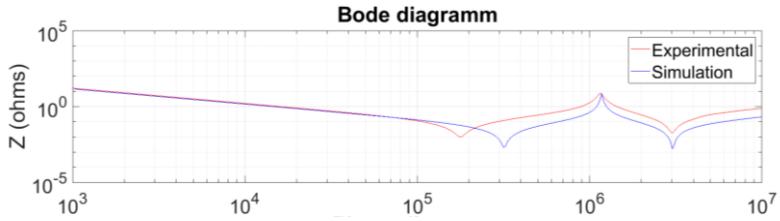

Figure 7:Bode diagram of the power circuit

While the project progressed, higher power GaN devices became available and 650 V, 120 A GaN devices could be used for the 2nd generation power boards. The power board has been designed as shown in fig. 8 (left and center). The topology of the board is almost the same as on the prototype, only an extra power device has been added which acts as series switch (functionality explained in chapter 3.3).

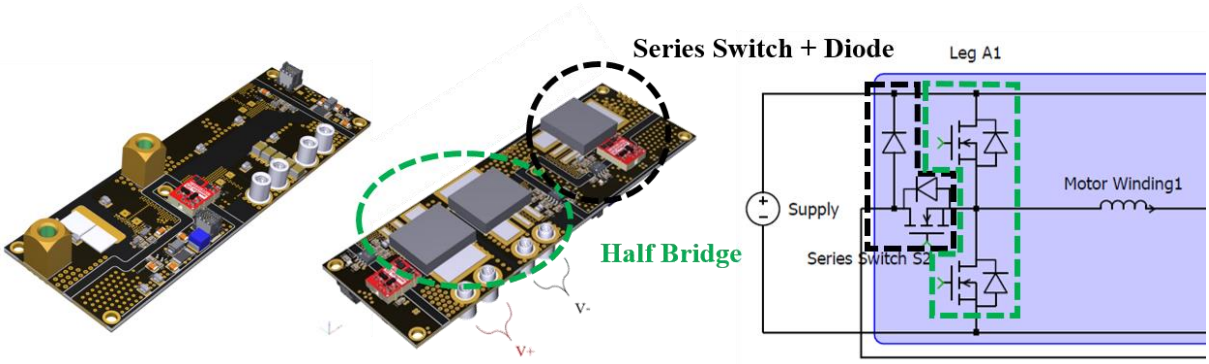

Figure 8: Power PCB with GaN device, top- (left) and bottom side (center), electrical circuit of one leg (right)

3.3 Series-independent Winding Reconfiguration

In this section, a six-winding EM is used to explain the winding reconfiguration principle. Its windings are independent from each other, meaning there is no star point, which enables a free choice of the machine winding configuration. Fig. 9 shows the implementation for one of the three phases, i.e. for two windings.

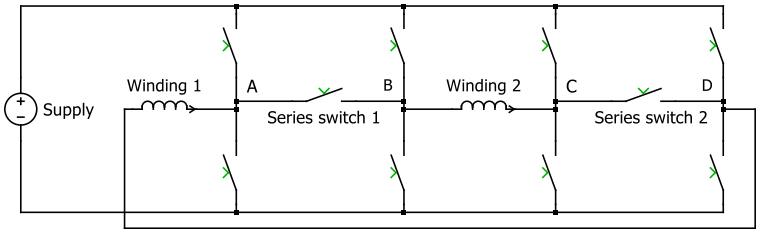

Figure 9: Switch matrix for one phase (winding pair)

The two windings are connected to the supply by means of a switch matrix, comprising two full bridges and two series switches, depicted as contactors, and each machine winding is represented by a single inductor. The matrix is able to interconnect the windings in series, or to connect each winding independently to the supply. In the series configurations, either series switch 1 or 2 is closed. Hence, the current in the series-connected windings can be controlled by means of two phase legs only, which is advantageous with respect to switching losses in the phase legs.

In the independent configurations, the winding currents are controlled individually. Nevertheless, due to the symmetric construction of the motor, both currents will in principle be controlled to the same value.

In a first implementation of this concept [7], a single series switch was used, and the reconfiguration was applied depending on the actual speed of the motor. However, this way of operating has to include a certain margin for varying supply voltage, stator impedance, and magnetic field strength in the machine. Additionally, once the independent configuration is used, it applies during a complete cycle of the voltage wave of the machine phase, although in the sections close to a zero crossing the series configuration could still be used. Finally, with only a single series switch available, the loading of the four phase legs is asymmetric, as always the same two legs are disabled in series operation.

Therefore, in the present work it was decided to extend the reconfiguration concept: when possible, a series configuration is used, and only where necessary (starting at the peak of the voltage wave applied to a machine phase) the windings are controlled independently. Also, in order to spread the losses more evenly over the phase legs, a second series switch was introduced, as already shown in fig. 9. As an ultimate refinement, the PWM patterns in the independent configuration are shifted 180 degrees with respect to each other, thereby minimizing the net torque ripple in the machine.
Due to the reconfiguration, the system order changes during operation: in the series mode only one current per phase needs to be controlled, but in the independent mode two currents have to be regulated. The resulting control method for one phase is depicted in fig. 10. As shown, the switching on/off of the Difference Current controller (by definition zero in the series configuration) is governed by a binary signal derived from the output of the Sum Current controller (the desired winding current): once the demanded voltage for the series connection becomes too large in view of the DC link voltage, the configuration is changed to independent, the Difference Current controller is enabled, and the controller gain halved in order to avoid a transient in its output due to the changed load configuration.

For controlling all three phases, the sum currents will be transformed to the d-q-0 frame by means of the Park transformation. For brevity, this approach, which is quite standard for the control of three-phase machines, will not be detailed further in this paper.

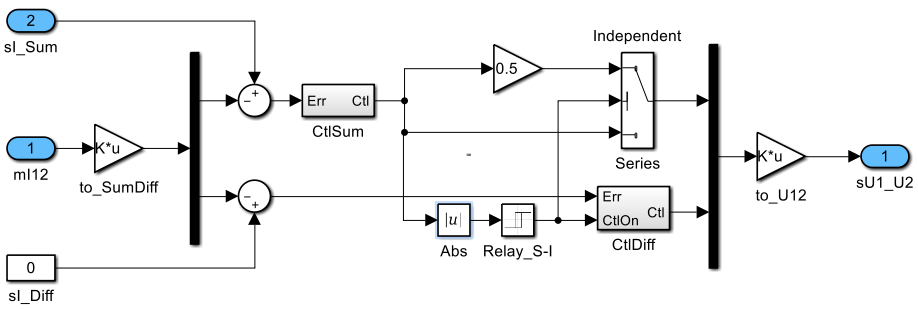

Figure 10: Control system for one phase (winding pair).

3.4 Simulation Results of Winding Reconfiguration

A first result of the control concept discussed above is shown in fig. 11.

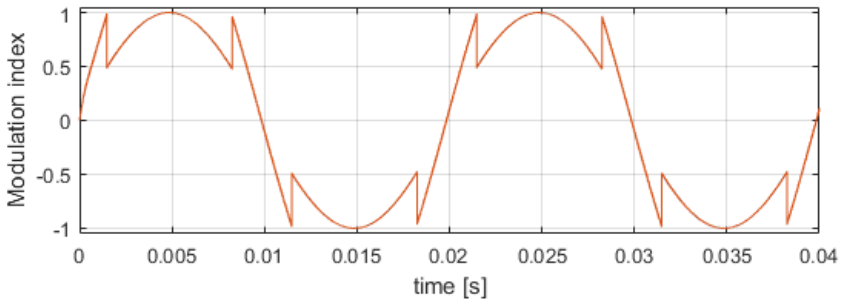

Figure 11: Simulation result for one phase when generating a sine-wave voltage.

Here, the circuit is generating a sine wave voltage across one winding pair. As shown, once the modulation index for the series connection reaches 1 or -1, the configuration is changed to independent and correspondingly the modulation index used to generate the PWM signals is halved. Once the resulting index drops below 0.5, the series configuration is restored. The shape of the individual currents in a similar situation is shown in fig. 12. It can be seen that each current follows the set-point, and the ripple of the sum current remains low in both the series and independent configurations.

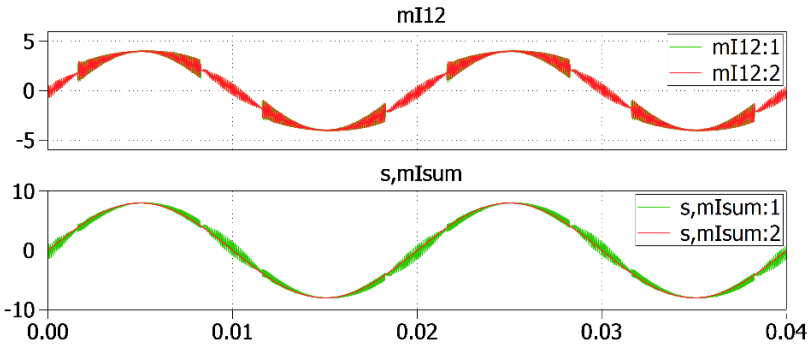

Figure 12: Simulation result for one phase when generating a sine-wave voltage and current. Individual currents (top) and set point and actual sum current (bottom) Horizontal scale: [s], vertical: [A].

3.5 Industrialization Potential of GaN Devices

GaN is a young and emerging technology, which has a lot of advantages and great potential for automotive applications [3, 4]. With increased switching frequency and low losses, it allows to build very efficient and compact power converters and inverters. Soon the cost of such a device will be similar to Si and much cheaper than SiC [5]. Moreover, as it is a non-mature technology, technical improvements are to be expected, whether for the device performance itself (e.g. current capability and reliability) or the manufacturing process. The prediction of CEA is that SiC devices will stay at the foreground for high voltage (> 1 kV) applications. However, GaN technology will in a few years dethrone low voltage (< 1 kV) technologies which have been installed for quite some time in power electronics such as IGBTs, Cool-MOS etc.

Interestingly it was noticed during the power board development, that auxiliary components such as passive components, drivers, measurement probes etc. are not always adequate for the use with GaN devices and progress has to be made also in those fields, without which, the use and development of GaN-based inverters remains difficult.

4 Transmission

For the transmission two options were considered in the project. The first option is a fixed ratio, single speed transmission. The second option is a dual ratio, switchable transmission. Several aspects were considered to help making the decision:

- Overall powertrain efficiency during type approval cycles: no clear winner between the two options
- A dual ratio transmission with adapted ratios provides higher launch torque in first gear and higher top speed for the same motor speed in second gear: this benefits the projects demonstrator that has limited motor torque due to the current limitations of the available GaN devices.
- Market demand: some customers prefer a dual ratio transmission for EV powertrains for particular reasons (e.g. gradeability, large difference between empty vehicle mass and fully loaded vehicle mass).

As for the projects targets advantages of dual ratio transmission surpass disadvantages, it was decided to develop a dual ratio, switchable transmission. The ratios of the transmission are 21.65 for the first gear and 12.18 for the second gear which leads to a ratio step of 1.78

The development process is described in the following: With the help of the gear synthesis software PlanGear from ZG, different gear configurations could be elaborated on the level of stick diagrams. Out of 34 possible configurations which fulfil the drivetrain's requirements, the four configurations with the highest efficiencies were depicted for further investigation. These configurations were then evaluated with respect to expected costs and overall size. Finally, the combination of a Ravigneaux planetary system and a pair of cylindrical gears was identified as most promising solution. In a next step, gear and bearing dimensioning was elaborated with the use of the transmission calculation software MASTA by SMT. Shaft and bearing loads were based on highly demanding drive cycles. Fig. 13 illustrates the design process of the gear and bearing configuration.

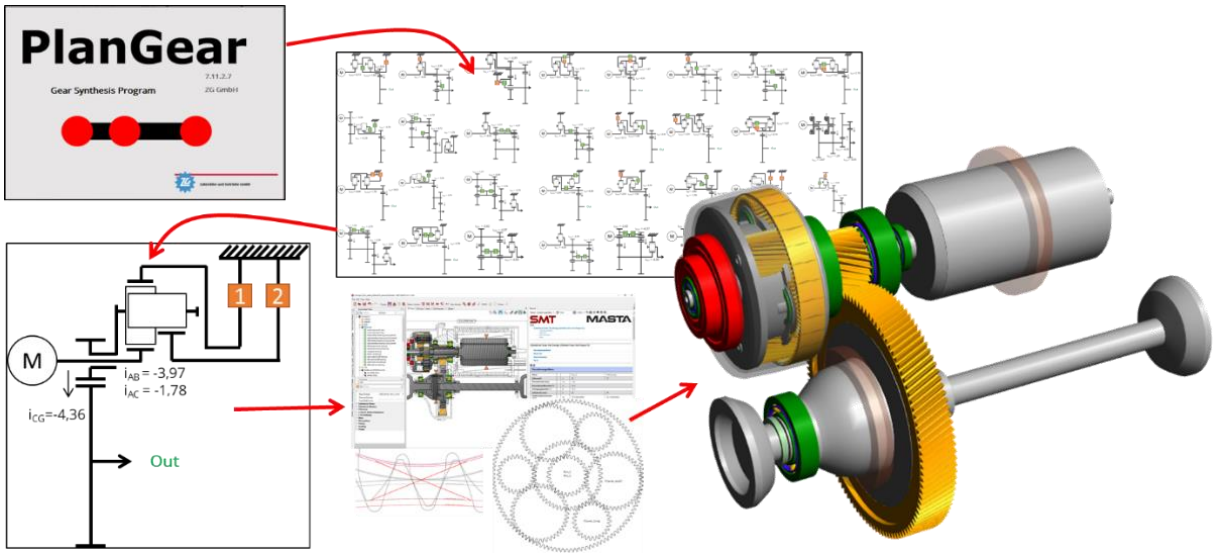

Figure 13: From gear synthesis to simulation model

Several configurations were reviewed whilst taking the manufacturing methods for parts and the way of assembly of the powertrain into account. Subsequently, detailed gear and bearing lifetime calculations based on highly demanding drive cycles were performed. Load-capacity, efficiency, weight and costs of possible bearing arrangements were evaluated and compared. Where possible, ball bearings are applied to reduce transmission losses. Once the transmission layout was known, the oil routing was developed to assure all bearings and gears are lubricated sufficiently.

5 Module Assembly

5.1 Housing and Cooling

One of the ambitions of this project is to obtain a highly integrated, compact electric powertrain. The integration of motor, inverter and transmission into a single unit simplifies the powertrain assembly in the vehicle. Furthermore, the integration reduces the cost of interfacing by eliminating connectors, cables and covers. At the same time a modular approach should allow exchanging (a part of) the motor, inverter or transmission for repair.

From different layouts the consortium chose an arrangement where the inverter boards are placed around the drive shaft as can be seen in fig. 14 (left). This choice provides a compact unit with the best balance of length (L), width (W) and height (H).

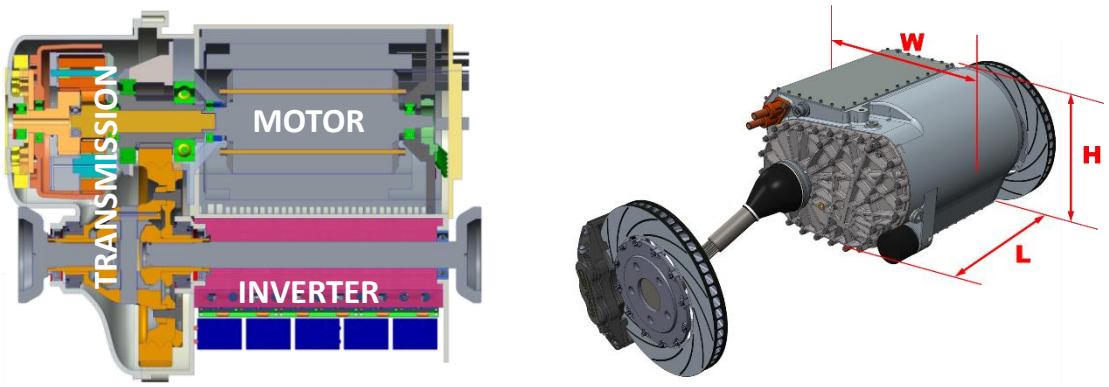

Figure 14: Cross section of chosen layout (left) and main dimensions of sample powertrain (right)

An important feature of the integrated housing is the cooling of both motor and inverter. Prior experience has learned that a too high back pressure in the cooling system requires a fairly high coolant pump power for the required flow. For this reason the cooling subsystem puts the cooling of motor and inverter in parallel. The motor cooling itself uses several parallel channels.

5.2 Resulting Specifications

Table 1: Module specifications

Parameter	Value
Maximum overall width, length & height (W x L x H as in fig. 14, right)	405 x 513 x 275 mm
Max. Power at wheels	134 kW
Max. Torque at wheels	3100 Nm
Required battery DC voltage	320 V

6 Holistic Design Approach

The best electric machine, the best inverter and the best transmission do not necessarily combine to the best drive module. This is because properties of fully electric drive modules result from multi-physical interaction of the powertrain components (electrical, mechanical and thermal). A design of the components with regard to the performance on vehicle level is necessary in order to find a global optimum for a specified vehicle and fixed driving requirements [8]. Furthermore, the control system design for the drive module is important to consider because it can increase the interaction between different subsystems but also be a remedy for unwanted interaction.

Parallel to the engineering of the drive module, a design process is being developed which aims to identify the best combination of components for the demonstrator vehicle. “Best” herein means the ideal compromise between costs, efficiency, performance, weight, volume and complexity. The result is an iterative and computational intensive process, which involves detailed component modelling of transmission, electric machine and inverter, as well as vehicle longitudinal dynamics simulation in order to evaluate the components on system level (fig. 15).

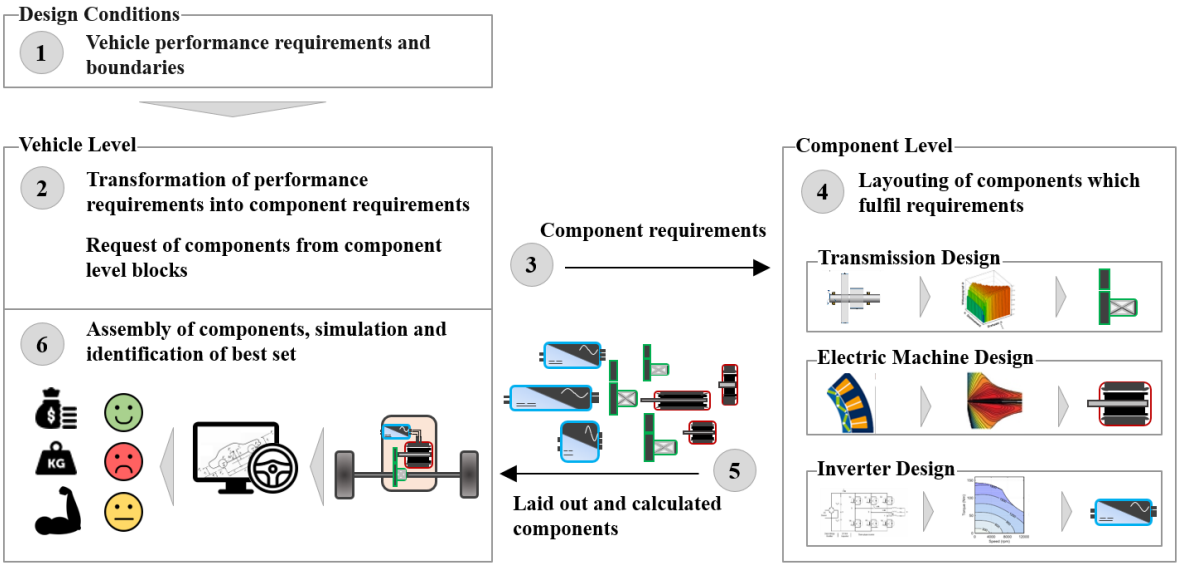

Figure 15: Holistic design process of electric drive modules

In the first step, the requirements on vehicle level (e.g. acceleration from 0 to 60 km/h in 3.9 seconds) are broken down to component level (1 & 2). This results in a set of component requirements such as torque, power, gear ratio, etc. (3). The component level calculation blocks layout and design components to fulfil the requirements and return the results (4 & 5). The components are virtually assembled and the performance on system level is evaluated through numerical and analytical vehicle simulations. By weighting of different design criteria such as costs, performance, weight, etc., the best set of components for the specified target vehicle is found (6). As this study is ongoing and targeted to complete in Summer 2019, no resulting drive module specification can be shown yet. However, the outcome of this design study is not only a suitable specification for drive modules for the Volvo C30e, but also to give insights into the component interaction between electric machine, inverter and transmission. The following findings have been gained until now during the development and usage of the presented design environment:

- **Electric Machine:** High speed EM generate power over high speeds and therefore do need less winding current than low speed EM. Ohmic losses in the windings are reduced while the iron losses slightly rise. However, the savings in winding losses surpass the additional iron losses and the machine is more efficient.
- **Inverter:** Classical Si-based inverters are still a good choice for slow to medium switching frequencies. At high switching frequencies, GaN and SiC provide a suitable characteristic. The latter option leads to very compact Inverters, as the size of the DC-link capacitor can be reduced with higher switching frequencies.
- **Transmission:** With higher maximum EM speeds, higher reduction ratios are required and the transmission gets bigger and less efficient. For high reduction ratios, more complex topologies show advantages compared to simple spur gear designs.
- **Module Level:** A module based on a high speed electric machine as presented above is more efficient and compact compared to conventional modules, even though the transmission itself is not. The drawbacks on the transmission side are overcompensated by the advantages on the machine and inverter side. However due to high switching frequencies, conventional IGBTs produce high switching losses and thus wide bandgap materials (GaN and SiC) should be used. Based on the current cost structures the use of these materials results in a higher price on module level.

Acknowledgments

The authors want to express their gratitude for the opportunity of this research to the ModulED project (http://moduled-project.eu/), co-funded by the European Union under H2020 programme.

References

[1] W. Todts, *CO_2 Emissions from Cars: The facts,* European Federation for Transport and Environment AISBL, 2018

[2] Benedikt Vogel, *Electric Power Package with High Efficiency,* Swiss Federal Office of Energy SFOE, 2019

[3] Adrien Letellier et al., *Gallium Nitride Semiconductors in Power Electronics for Electric Vehicles: Advantages and Challenges.* 2015 IEEE Vehicle Power and Propulsion Conference (VPPC), ISBN 978-1-4673-7637-2, Montreal, 2015

[4] Srabanti Chowdhury*, GaN Electronics for Next Generation Cars,* https://tec.ieee.org/newsletter/november-december-2014, accessed on 2018-10-15

[5] S. Reese et al., *How Much Will Gallium Oxide Power Electronics Cost?* Joule, 2019, ISSN 2542-4351, https://doi.org/10.1016/j.joule.2019.01.011.

[6] GaN Systems Inc., *GS66516T Top-side cooled 650 V E-mode GaN transistor - Preliminary Datasheet*, https://gansystems.com/gan-transistors/gs66516t/, accessed on 2019-03-13

[7] Thomas Gerrits, C.G.E. Wijnands, J.J.H. Paulides, J.L. Duarte. *Electrical gearbox equivalent by means of dynamic machine operation*. Proceedings of the 2011 14th European Conference on Power Electronics and Applications.

[8] Albert Albers et al., *Software supported development process of a Battery Electric Vehicle powertrain considering the efficiency,* VDI-Berichte, 2276(2016), 321-337

Authors

Jonas Hemsen studied communication sciences and automotive engineering, graduating in 2017. Parallel to his studies, he worked in the Electric/Electronics department as well as in the battery development of Adam Opel AG. Since 2017 Jonas is a PhD candidate at the institute of automotive engineering, focussing on electric drivetrain design and simulation. He is also a lecturer in the fields of “alternative and electrified vehicle propulsion systems”.

Daniel Kieninger studied Automotive Engineering at the University of Stuttgart. He graduated in 2010 (Dipl.-Ing.) and is currently working as a PhD candidate in the position of team leader at the ika. Being team leader of the drivetrain department he is acquiring and organizing projects focusing on hybrid and battery-electric vehicles. His specialization is the assessment, simulation, and function development of alternative vehicle propulsion systems.

Lutz Eckstein is director of the Institute for Automotive Engineering (ika) at RWTH Aachen University. The institute has more than 140 employees and spans its research scope widely across all vehicle related fields: Electronics, chassis, body, drivetrain, thermal management, acoustics, autonomous driving, future vehicle concepts and -strategy. He is furthermore chairman of the Advisory Board of fka GmbH, chairman of the “VDI Advisory Board Vehicle and Traffic Technology” and member of SAE.

Mathias Lidberg is an Associate Professor in Vehicle Dynamics at Chalmers University of Technology. Prior to PhD studies, he was an Engineering Analyst and Project Manager with Mechanical Dynamics Inc. (now Hexagon). His primary research area is integrated powertrain and chassis control. He is also teaching and supervising graduate and post-graduate students. Furthermore, Dr. Lidberg is the co-founder of one start-up company in the automotive area.

Henk Huisman is Associate Professor in the Department of Electrical Engineering at Eindhoven University of Technology (TU/e). His research and teaching concerns precision power amplifiers, motor drives, and isolated power converters. As Assistant Professor, Henk previously worked on the analysis and design of high-precision power amplifiers and resonant power converters. He has authored or contributed to 34 conference papers, 10 articles, 6 patent publications and 2 book chapters, on multiphase series-resonant power converters, flywheel applications, and various other topics.

Elena A. Lomonova was born in Moscow, Russia. She received the M.Sc. (cum laude) and Ph.D. (cum laude) degrees in electromechanical engineering from Moscow State Aviation Institute, Moscow, in 1982 and 1993, respectively. Since 2008, she has been a Full Professor and the Head of Electromechanics and Power Electronics Group at the Eindhoven University of Technology, Eindhoven, The Netherlands. She has been involved in electromechanical actuator designs, powertrain and energy conversion systems, and optimization and development of advanced mechatronic systems.

Daniel Oeschger graduated as automotive engineer (B. Sc.) at Bern University of applied sciences (BFH) in 2009. Since 2011 he works for BRUSA Elektronik AG. He started as predevelopment test engineer for mechanical issues. He optimized the component cooling of the NLG6 22kW fast charger, For the DMC7 (>100.000rpm high-speed inverter). Since 2015 he is developing new motor types with FLW (Formed Litz Wire) technology. He invented, tested and patented a new solution for FLW mass production.

Charley Lanneluc is the project manager and European coordinator for the ModulED project. After graduating in electrical engineering, he worked at the national society of French railway system as a signal processing engineer, specialised on battery management systems. Later he joined CEA as a power electronics and embedded systems engineer currently working in the fields of power electronics design, modelling, simulation and testing of electric circuits.

Olivier Tosoni graduated as a physical engineer at the Ecole Polytechnique (Paris) and defended his PhD on thin-film solar cells in the University of Grenoble in 2013. Since 2014 he has been working at CEA on magnetic materials and components. His activities include material synthesis and characterization, with an emphasis on sintered and injected NdFeB magnets, and design/prototyping of various magnetic systems (captors, motors, energy harvesting devices,…)

Patrick Debal graduated as Master of Science in Mechanical Engineering at the University of Leuven, Belgium in 1985. He held several positions in research and development before joining Punch Powertrain in 2006. At Punch Powertrain Patrick has been in charge of hybrid powertrain development. He is currently Powertrain Expert in the Research, Technology and Advanced Development group.

Michael Ernstorfer studied Mechanical Engineering at TU Munich. He joined ZG - Zahnrad and Getriebe GmbH – in 2008 and became Managing Director in 2011. ZG is specialized in gear technology and delivers innovative gears to OEMs and Tier 1 automotive suppliers as well as to other industries. The company employs around 40 people.

Rémi Mongellaz joined Siemens PLM Software in 2013 as an Electromechanical Engineer. He works on e-powertrain modeling for various electromobility research projects. He also contributes to the development of the electrical libraries and capabilities of Simcenter Amesim (an integrated simulation platform for multi-domain mechatronic systems simulation).